Hybrid luminescent/magnetic nanostructured porous silicon particles for biomedical applications

Álvaro Muñoz-Noval,[a] Vanessa Sánchez-Vaquero,[a] Vicente Torres-Costa,[a] Darío Gallach,[a] Vicente Ferro-Llanos,[b] José Javier Serrano,[b] Miguel Manso-Silván,[a] Josefa Predestinación García-Ruiz,[a] Francisco del Pozo,[b] and Raúl J. Martín-Palma[a]

[a]Universidad Autónoma de Madrid, Centro de Investigaciones Biomédicas en Red: Bioingeniería, Biomateriales y Nanomedicina (CIBER-bbn), Departamento de Física Aplicada, Departamento de Biología Molecular, 28049 Cantoblanco, Madrid, Spain

[b]Universidad Politécnica de Madrid, Centro de Investigaciones Biomédicas en Red: Bioingeniería, Biomateriales y Nanomedicina (CIBER-bbn), and Centro de Technología Biomédicas, Grupo de Bioingeniería y Telemedicina, Spain

Abstract. This work describes a novel process for the fabrication of hybrid nanostructured particles showing intense tunable photoluminescence and a simultaneous ferromagnetic behavior. The fabrication process involves the synthesis of nanostructured porous silicon (NPSi) by chemical anodization of crystalline silicon and subsequent in pore growth of Co nanoparticles by electrochemically-assisted infiltration. Final particles are obtained by subsequent sonication of the Co-infiltrated NPSi layers and conjugation with poly(ethylene glycol) aiming at enhancing their hydrophilic character. These particles respond to magnetic fields, emit light in the visible when excited in the UV range, and internalize into human mesenchymal stem cells with no apoptosis induction. Furthermore, cytotoxicity in in-vitro systems confirms their biocompatibility and the viability of the cells after incorporation of the particles. The hybrid nanostructured particles might represent powerful research tools as cellular trackers or in cellular therapy since they allow combining two or more properties into a single particle.
© 2011 Society of Photo-Optical Instrumentation Engineers (SPIE). [DOI: 10.1117/1.3533321]

Keywords: Porous silicon; nanoparticle; human mesenchymal stem cell; citotoxicity; multifunction.

Paper 10466RR received Aug. 24, 2010; revised manuscript received Nov. 14, 2010; accepted for publication Dec. 8, 2010; published online Feb. 2, 2011.

1 Introduction

Semiconductor based nanostructures with controlled composition and dimensions are increasingly being used in several biological applications such as cellular and molecular imaging, cell labeling and tracking, multiplexed analyses, and DNA detection as recently reviewed.[1,2] The typical size of nanoparticles, comparable to that of many common biomolecules, makes them appropriate for the development of hybrid nanostructured systems.[3,4] In this frame, quantum dots possess many advantages over organic fluorophores; size tunable fluorescence emission, large absorption across a wide spectral range, narrow emission spectra, and high levels of brightness and photostability.[5,6]

In addition to this, magnetic nanoparticles are receiving increased attention given their potential use in medicine. Nanoparticles with tailored magnetic properties have found functionality in the manipulation of biological materials in immunoassays,[7] targeted delivery of therapeutic compounds,[7] controlling cell–cell interactions,[8] hyperthermia treatments,[3] or as magnetic resonance imaging contrast agents.[9] Aiming at the integration of nanostructures into biological systems, chemical modifications can be induced in order to boost biocompatibility and/or to enhance aqueous solubility. Chemical grafting groups, such as amines or carboxylic groups[10] can be used to bind selected biomolecules (proteins,[11] polypeptides,[12] oligonucleotides,[13] etc.) to nanoparticle surfaces. Such chemical grafting groups can be alternatively conjugated through an hydrophilic poly(ethylene glycol) (PEG) complex thus providing new hybrid multifunctional nanostructures.[14]

Within this context, porous nanostructures offer the advantage of increased surface area, resulting in enhanced surface activity.[15] This property enormously facilitates bioconjugation for targeting or directed delivery[16] and biosensing.[17] Nanostructured porous silicon (NPSi) formed by photoelectrochemical etching[18] has emerged among the functional porous semiconductors, whether as a gas sensor,[19] a photoluminescent probe,[20] or as a therapeutic agent through near infrared irradiation.[21] Furthermore, nanoparticles can be infiltrated into NPSi, thus imparting additional properties to the resulting hybrid system (magnetic metals in NPSi for designing storage devices,[22] or high conductivity transition metals for electronic contacts[23]). In this work, Co-infiltrated NPSi particles are prepared with the aim of providing multifunctional magnetic/fluorescent materials with a PEG coat. Though II-VI semiconductors have been previously proposed for this multifunctional purpose, we herein introduce a scheme based on NPSi, a form of silicon with reputed biocompatibility in several tissues.[4,24,25] Furthermore, to open the path for biofunctionalization through PEGylation cascades, a PEG–NPSi conjugate is formed leading to hybrid

Address all correspondence to: Álvaro Muñoz-Noval, Departamento de Física Aplicada, Departamento de Biología Molecular and Centro de Investigaciones Biomédicas en Red: Bioingeniería, Biomateriales y Nanomedicina (CIBER-bbn), Universidad Autónoma de Madrid, 28049 Cantoblanco, Madrid, Spain. Tel: +34 91 4974919; E-mail: alvaro.munnoz@uam.es.

1083-3668/2011/16(2)/025002/8/$25.00 © 2011 SPIE

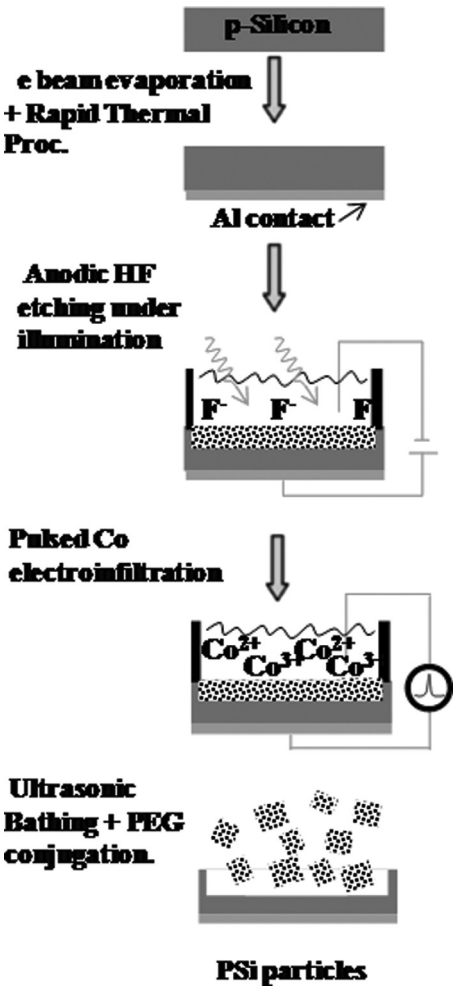

Fig. 1 Schematic process followed for the preparation of hlmNPs.

luminescent/magnetic nanostructured particles (hlmNPs). To assess on their biocompatibility and nontoxicity, internalization assays are performed in human mesenchymal stem cells (hMSCs), which are afterward the subject of a MTT (3-[4,5-dimethylthiazol-2-yl]-2,5-diphenyl tetrazolium bromide) cytotoxicity assay. This assay is based on the ability of viable cells exposed to different types of nanoparticles[5,6,26] to convert in the mitochondria a tetrazole yellow salt into a reduced purple formazan. This reduction takes place only when succinate dehydrogenase enzymes are active so that only viable cells with no alterations induced by nanoparticles exhibit a color change.

2 Experimental

2.1 *Fabrication of Hybrid Luminescent/Magnetic Nanostructured Particles*

The complete procedure for the fabrication of hlmNPs is schematically represented in Fig. 1. Silicon substrates (p-type boron-doped, orientation <100> and resistivity 0.01–0.02 Ω cm) were prepared for the subsequent electrochemical processing by depositing an Al contact by electron beam evaporation and rapid thermal annealing (Fig. 1, step 1). NPSi layers were fabricated by the electrochemical etch in 1:1 HF (48 wt%):ethanol (98 wt%) solutions of the Si wafers. NPSi layers with thickness ranging from 40 to 50 μm were obtained under illumination (100 W halogen lamp) using current densities from 80 to 110 mA/cm^2 (Fig. 1, step 2) during 400 s.

Table 1 Composition of the Watts bath used for the electroinfiltration of Co into NPSi.

Component	Concentration
$CoSO_4 \cdot 7H_2O$	0.2M
$CoCl_2$	0.05M
Na-Sacharine	5 g/l
H_3BO_3	0.4M
H_2SO_4	1mM
water	——

Subsequent electroinfiltration of Co in the current-equilibrium pulsed mode was performed by immersion of the NPSi layers in a Watts bath using Co salts and suited catalytic converters (Fig. 1, step 3).[27,28] The composition of the Watts bath is shown in Table 1.

Co-infiltered NPSi particles were obtained by 20 min sonication and dispersion. The final conjugation step was immediately carried out by immersion in a poly(ethylene glycol)-600/toluene (1% vol) solution (Fig. 1, step 4) as previously illustrated.[20] These particles were exposed to the atmosphere for over 1 h for stabilization of their physico-chemical properties before characterization.

Finally, four cycles of centrifugation (12 krpm, 5 min), supernatant removing and re-dispersion in ethanol solution (sonication, 10 min) were applied to the resulting particles.

2.2 *Characterization*

Morphological characterization was performed by a combination of scanning electron microscopy (SEM) and transmission electron microscopy (TEM). SEM characterization was performed in a Hitachi S-3000N SEM equipped with a conventional thermionic filament and an operating voltage of 20 keV. Qualitative chemical information was retrieved by energy dispersive X-ray analysis (EDX). TEM images were acquired using a JEOL-JEM1010 (100 KV) microscope.

Magnetic characterization by Alternating Gradient Field Magnetometry (AGFM) was performed in a Micromag 2900 AGFM System (Princeton Measurements Corporation). Nine measurements were taken for each sample. Measurements were carried out applying a magnetic field from − 100 mT to 100 mT, a time pass of 100 ms, and a field pass of 800 μT.

Luminescence spectra were acquired in an AMINCO Bowman Series 2 Luminescence Spectrometer (SLM Instruments INC), equipped with a 250 W Xenon Lamp. Measurements were obtained with a detector voltage of 700 V and an excitation wavelength of 400 nm. Spectra at successive atmosphere exposure times were acquired, from freshly conjugated

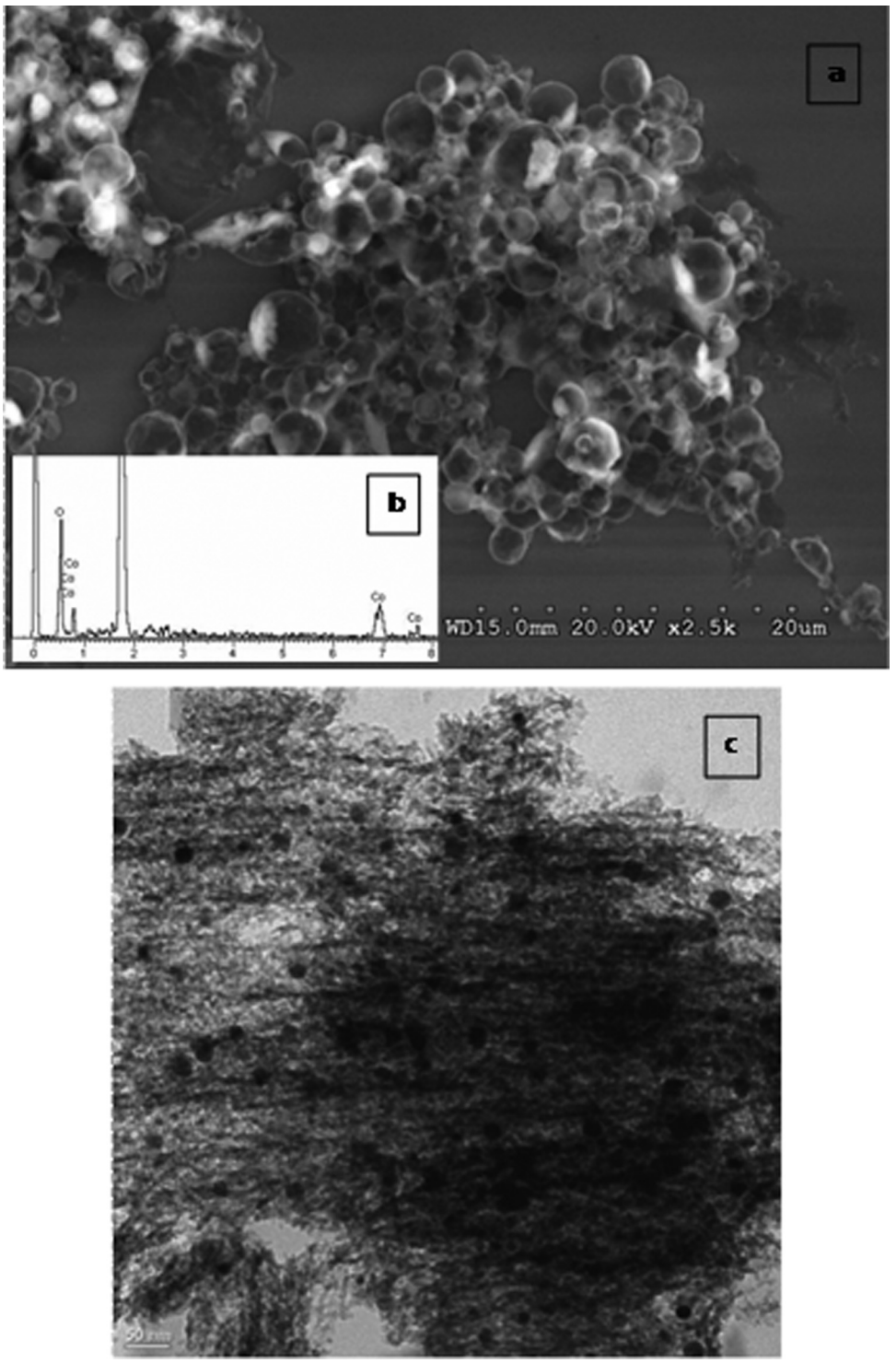

Fig. 2 (a) Morphology of hlmNPs immediately after PEG conjugation showing spherical nanostructured particles as observed by SEM. (b) A typical EDX spectrum from a pre- tore layer of the Co-infiltrated NPSi. (c) TEM micrograph of hlmNPs showing a NPSi shell and a multicore of Co nanoparticles.

hmlNP samples to 72 h atmosphere exposed in intervals of 24 h.

2.3 *Cell Culture*

The hlmNPs were further treated for the different bioassays as follows. Aliquots of 300 μl (concentration 25 g/l) of hlmNPs were centrifuged for 10 min and rinsed in Phosphate buffered saline (PBS)(0.5 ml) three times to remove any traces of toluene and to equilibrate pH. Then, rinsing was repeated three times using 1 ml of Dulbecco's Modified Eagle Medium (DMEM, Gibco) and centrifugations as above. Finally, samples were left overnight immersed in DMEM without centrifugation to improve pH stability. Particles were then exposed to hMSCs

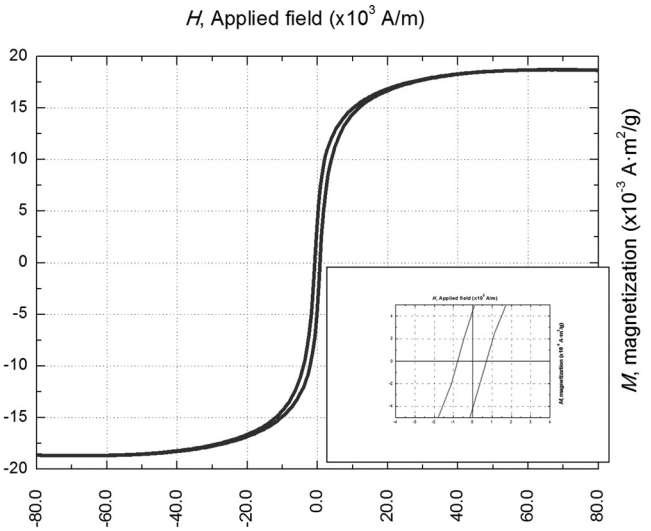

Fig. 3 AGFM hysteresis loop of hlmNPs obtained at 298K. Values have been normalized for an average weight of hlmNPs in solution. The inset shows the coercivity field.

plated on 0.5% gelatin-coated cover slips. Two to four ml of human bone marrow was extracted from healthy donors for the isolation and expansion of hMSCs.[29,30] Cells were collected by centrifugation on 70% Percoll gradient and seeded at 200,000 cm^{-2} in DMEM-low glucose (LG) supplemented with 10% Fetal Bovine Serum (FBS) (Sigma). The hMSCs were used to analyze whether or not particles are internalized by cells and if so, determine their potential toxicity. To this end 15,000 cells were seeded on 0.5% gelatin-coated cover slips (bovine skin, Sigma). The hMSCs were incubated with DMEM-LG plus 10% FBS for 24 h and then exposed (except for controls) to 0.15 mg/ml hlmNPs at 37ºC in 5% CO_2 atmosphere, during periods of 4 and 72 h. Then, adhered cells were washed twice with PBS and fixed in 3.7% formaldehyde in PBS for 20 min at room temperature. After fixation, cover slips were washed twice with PBS, samples dehydrated with absolute ethanol (Merck) and mounted with Mowiol/Dabco (Calbiochem). Cells were visualized in a fluorescence vertical microscope (OLYMPUS IX81, UV excitation at 350 nm) coupled to a CCD camera.

2.4 *Cytotoxicity Assay*

The possible cytotoxicity of particles in the culture of hMSCs was determined after 4 and 72 h incubation in DMEM-LG evaluating cell viability by MTT (3-[4,5-dimethylthiazol-2-yl]-2,5-diphenyl tetrazolium bromide) colorimetric assay (Sigma). A solution of 20 μl of 5 mg/ml MTT in PBS was added to each well of a M96 plate where the cells were cultured with the hlmNPs. After 4 and 72 h incubation at 37ºC, medium was removed and 150 μl of MTT solution added [4 mM HCl, 0.1% Nonidet P-40 (NP40) in isopropanol (Merck)]. After 15 min of solubilization the absorbance of each sample was determined using a SmartSpec Plus BIO-RAD spectrophotometer at 590 nm with a reference filter of 620 nm. Each sample was tested in triplicate.

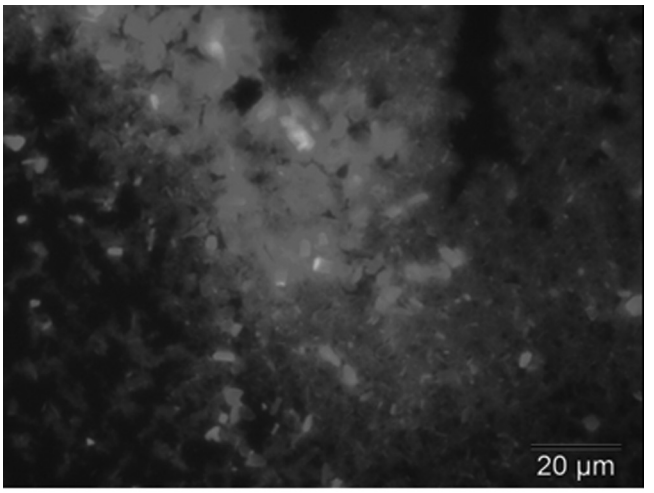

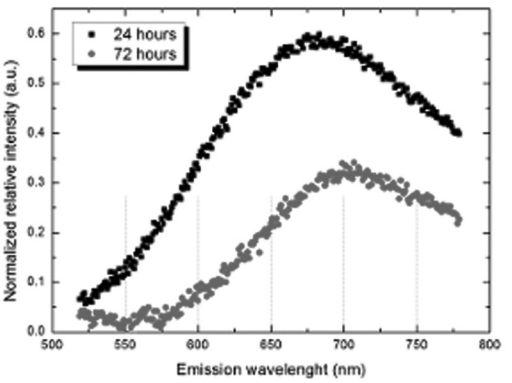

Fig. 4 (top) Fluorescence microscopy images of PEG conjugated, Co infiltrated hlmNPs after 24 h atmospheric aging (excitation 350 nm). (bottom) Evolution of luminescence of PEG conjugated, Co infiltrated hlmNPs (excitation 400 nm).

3 Results and Discussion

3.1 *Morphology and Composition*

The morphology of the hlmNPs was initially probed by using SEM. Figure 2(a) shows the morphology of hlmNPs immediately after PEG conjugation. The efficiency of NPSi-PEG conjugation has been previously demonstrated by using x-ray photoelectron spectroscopy.[20] These show a characteristic spherical shape with typical sizes ranging from 0.5 to 3 microns. In previous works,[31] we determined that porous silicon is composed of rounded Si nanocrystals with characteristic sizes ranging from 20 to 80 Å, embedded into an amorphous matrix and with no preferential orientation. Furthermore, we determined that the size distribution of the nanocrystals can be fitted to a Gaussian distribution centered at about 46 Å. Additionally, it was verified that the spherical shape of the hlmNPs is unaffected by the PEG conjugation process.[20]

The composition of pre-tore Co infiltrated NPSi layers was analyzed by EDX in cross sections in order to obtain an estimation of the Co infiltration homogeneity. Figure 2(b) reveals the presence of Si, O, and Co emerging from the NPSi host. Furthermore, cross-sectional EDX analysis shows that there is an in-depth Co concentration gradient from over 10% in weight close to the external surface to 1–2% in weight at the bottom of

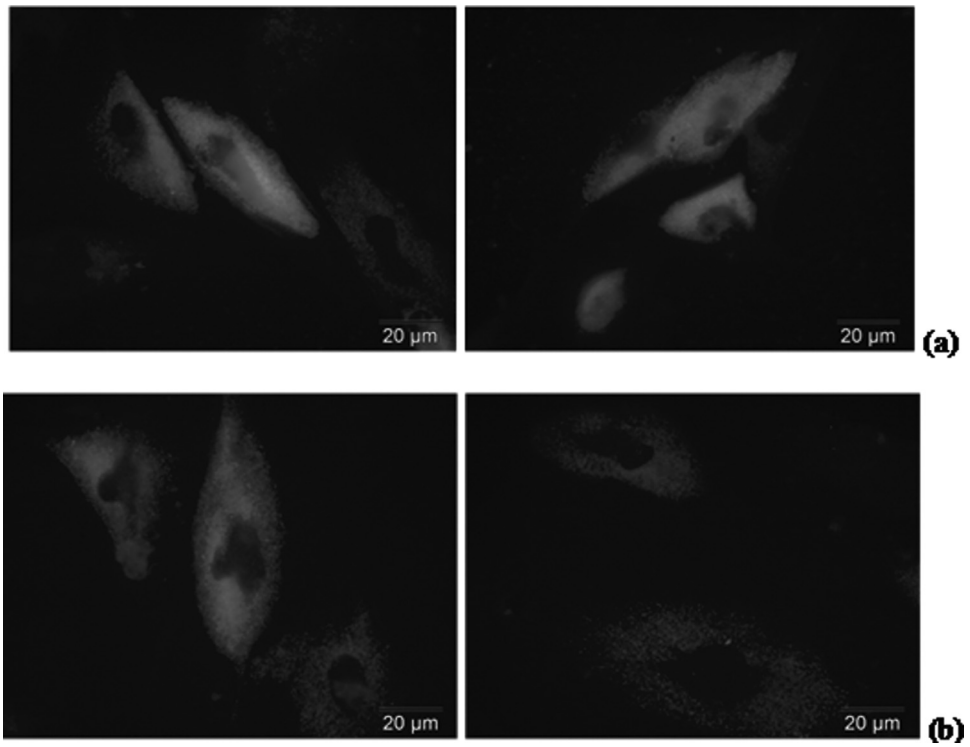

Fig. 5 Fluorescence images of internalized hlmNPs into hMSCs after (a) 4 and (b) 72 h (excitation 350 nm).

the layer (depths around 40 to 50 microns). The Co concentration was in average 3% in weight within the layer. Such low concentration is of significance for applications in the biomedical field given the potential toxicity of Co in the form of nanoparticles or in the ionic state.[32]

Additionally, the presence of electroinfiltrated Co structures into the NPSi particles is verified by TEM [Fig. 2(c)]. The micrograph shows a NPSi network with preferentially oriented along the horizontal direction. Relevantly, spherical Co nanoparticles with sizes ranging from 5 to 30 nm are formed into the pores. Furthermore, it is observed that the Co nanoparticles are arranged in a particular direction, in coincidence with the pore orientation. It is presumed that such orientation in the particle pores is originally normal to the Si wafer surface. TEM analysis confirms that the hlmNPs formed are in fact a composite of NPSi with a multicore of well dispersed Co nanoparticles. The shell role of NPSi is again considered as an attractive structure in order to reduce the potential toxicity of Co nanoparticles or ions.

3.2 *Magnetic Properties*

Dry hlmNPs were characterized in the AGFM. In order to study their magnetic properties independently of their concentration in solution, weight-normalized curves were obtained as shown in Fig. 3. The measured coercivity was about 9.3 Oe, a value comparable with low coercivity of bulk Co. Thus a nonsuperparamagnetic behavior is expected for hlmNPs in solution.[33] By comparing this value with that corresponding to Co thin films,[34] Co nanotubes,[35] or other Co structures and composites[36] it can be inferred that the dilution of Co in the NPSi leads to low coercivity values. This property is especially favorable for hyperthermia applications.[5,6] Regarding the magnetization, an average magnetic saturation of about $1.852 \cdot 10^{-2}$ $A.m^2.gr^{-1}$ was measured for the dried hmlNPs. Comparing this value with other saturation values of conjugated magnetic particles[3,37,38] it is clear that hlmNPs have a comparable saturation magnetization.

3.3 *Luminescence*

Luminescence from hmlNPs was initially observed by optical fluorescence microscopy for a qualitative determination of fluorescence emission (Fig. 4, top). A spectrometric analysis of luminescence was also carried out on PEG-conjugated samples in view of previous results demonstrating quenching inhibition in aged particles.[20] The aging of the samples under atmospheric exposure was studied by identifying the maximum emission wavelength and the intensity decay under optimized excitation at 400 nm (Fig 4, bottom). It is noted that the hmlNPs emit in the red region of the visible spectrum with emission maxima at 675 nm and 700 nm for 24 and 72 h atmospheric exposure, respectively. The emission peak shifts toward the infrared progressively and the emission in completely quenched after 72 h. Previous research[39,40] confirms that such quenching process is due to an oxidation of the emitting centers in NPSi. Simultaneously, surface silanol formation is the origin of the appearance of a new blue emission band centered at 490 nm. This secondary emission band, although less intense is more stable and can be exploited for environmental sensor engineering.[41] Such luminescence from hlmNPs will be the subject of further discussion in Sec. 3.4.

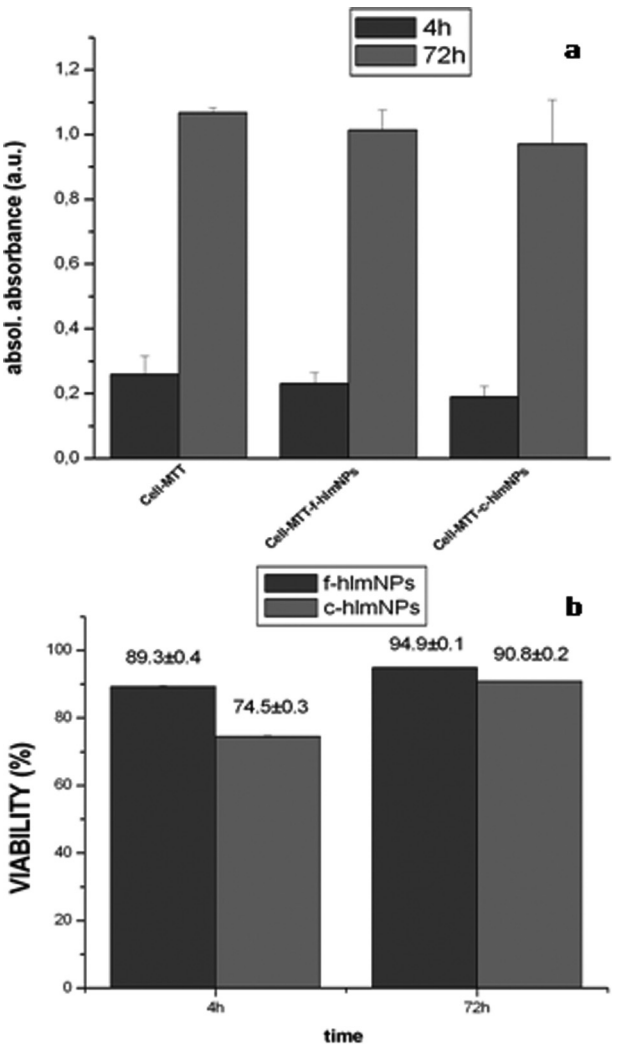

Fig. 6 (a) MTT cytotoxicity test results for the PEG-conjugated and PEG-free hlmNPs after 4 and 72 h of exposure. (b) Cell viability histogram relative to controls.

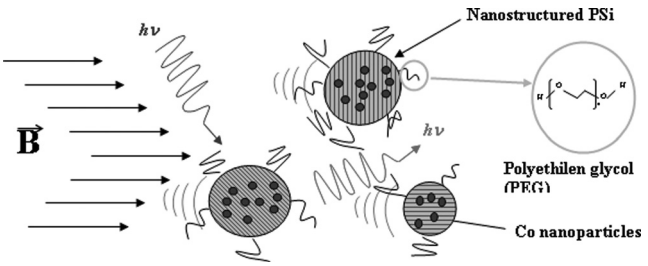

Fig. 7 Schematic representation of nanostructured porous silicon-based hlmNPs after conjugation. These comprise a nanostructured porous silicon (PSi) shell (striped particles) with a multicore of Co nanoparticles (solid blue particles). The hlmNPs have subsequently been conjugated with poly(ethylene glycol).

3.4 *In vitro Assays: Internalization of hlmNPs and Cytotoxicity Analysis*

hMSCs cultured in the presence of hlmNPs were observed by fluorescence microscopy. The experimental results show that hMSCs assimilate the particles present in the medium as derived from the preferential blue luminescence associated to hMSCs outlines observed in Fig. 5. The time required for particle-cell association is relatively low since images obtained after 4 h in culture allow a clear identification of the cell boundaries [Fig. 5(a)]. The localization of the nanoparticles is not homogeneous all over the cell. The fact that hlmNPs are depleted around the nuclear region (observe dark areas in the center of each cell) suggests that they are internalized and repulsively interacting with intermediate nuclear proteins. The different cultures intervals of 4 and 72 h [Fig. 5(b)] reveal that cells remain surface adhesive and show no apoptotic signs upon internalization of the particles. As we pointed out in Sec. 3.3, an important fact is that light emitted by the internalized particles is shifted with respect to as-prepared particles showing blue luminescence. These changes in luminescence are attributed to the rapid oxidation of NPSi in PBS medium, as described in Sec. 3.3.

In terms of biocompatibility, internalization is not the only parameter that needs to be considered. To determine the suitability of the hlmNPs for cellular studies, cytotoxicity in an in-vitro system was assessed to take into account the potential damage induced by delivery of Co nanoparticles or dissolved Co ions. With this objective MTT cytotoxicity assays were performed using concentration of 5 mg/ml of hlmNPs. The experimental results (Fig. 6) corroborate the viability of the cells in presence and incorporation of particles. In this case PEG-free and PEG-conjugated particles were studied.

The absorbance magnitude at the reference wavelength (620 nm, see section 2.4) is proportional to the viability of each sample. The absorbance of as-cultured hMSCs (Cell-MTT columns) is measured and used as a reference to compare with hMSCs cultured for 4 and 72 h in the presence of PEG-free hmlNPs (Cells-MTT-f-hmlNPs columns) and in the presence of PEG-conjugated hmlNPs (Cells-MTT-c-hlmNPs columns) [Fig. 6(a)].

The resulting percentage of viability rate (the absorbance reflects the viability of the cells) can be observed in Fig. 6(b). Both the conjugated and PEG-free particles showed positive viability rates near to those obtained for untreated control cells.

4 Conclusions

Nanostructured particles have been fabricated by the electroinfiltration of Co into porous silicon. Such combination attributes dual luminescent/magnetic behavior with intense luminescence as well as magnetic response. The resulting nanostructured particles have been subsequently conjugated with PEG, aiming at increasing the hydrophilic properties of the particles and opening the way to PEGylation mechanisms for the formation of targetable biomolecular-particle complexes. An overall graphic scheme of the synthesized particles is shown in Fig. 7. Dispersed Co cores within a NPSi shell conjugated with PEG respond to magnetic fields and emit in the visible when excited in the UV range. Such particles get internalized into hMSCs in less than 4 h of culture and can be considered as biocompatible as derived from cytomorphometric analysis.

Furthermore, MTT cytotoxicity assays in hMSC cultures prove the low toxicity of the particles, at least until working

concentrations of 5 mg/ml and up to 72 h of culture. Though initially red luminescence is quenched while a blue band appears by storing in solution, the particles remain functional photo emitters presumably in a longer time scale. Such time is considered to be enough to allow establishing protocols for cellular manipulation with external magnets and the possibility of simultaneous fluorescence control.

The possibility to fabricate silicon-based particles with dual magnetic/luminescent properties opens a wide range of possibilities for new research. On the one hand the versatility of the particles for biomedical applications could be increased by varying the size and/or composition of nanostructured porous silicon to obtain customizable luminescence (i.e., variable color) and magnetic behavior. Furthermore, given the versatility of silicon chemistry, several functional groups can be attached to the nanostructured porous silicon particles and various biomolecules immobilized in order to provide internal specificity within the cell (selective organelle labeling) or even applications in combined deep-tissue imaging.

Acknowledgments

We acknowledge funding from Comunidad de Madrid (Spain) under project "Microseres" and partial FEDER finance to CIBERbbn.

References

1. Y. Wang, Z. Tang, and N. A. Kotov, "Bioapplication of nanosemiconductors," *Mater. Today* **8** *(Suppl. 1)*, 20–31 (2005).
2. C. Jianrong, M. Yuqing, H. Nongyue, W. Xiaohua, and L. Sijiao, "Nanotechnology and biosensors," *Biotechnol. Adv.* **22**, 505–518 (2004).
3. Y. Xu, A. Karmakar, A. D. Wang, M. W. Mahmood, F. Watanabe, Y. Zhang, A. Fejleh, P. Fejleh, Z. Li, G. Kannarpady, S. Ali, A. R. Biris, and A. S. Biris, "Multifunctional Fe_3O_4 cored magnetic-quantum dot fluorescent nanocomposites for RF nanohyperthermia of cancer cells," *J. Phys. Chem. C* **114**(11), 5020–5026 (2010).
4. M. A. Walling, J. A. Novak, and J. R. E. Shepard, "Quantum dots for live cell and in vivo imaging," *Int. J. Mol. Sci.* **10**(2), 441–491 (2009).
5. F. Wang, B. W. Tan, Y. Zhang, X. Fan, and M. Wang, "Luminescent nanomaterials for biological labelling," *Nanotechnology* **17**, R1–R13 (2006).
6. W. Cai, D.-W. Shin, K. Chen, O. Gheysens, Q. Cao, S. X. Wang, S. S. Gambhir, and X. Chen, "Peptide-labeled near-infrared quantum dots for imaging tumor vasculature in living subjects," *Nano Lett.* **6**(4), 669–676 (2006).
7. H. P. Song, J. Y. Yang, S. L. Lo, Y. Wang, W. M. Fan, X. S. Tang, J. M. Xue, and S. Wang, "Gene transfer using self-assembled ternary complexes of cationic magnetic nanoparticles, plasmid DNA and cell-penetrating Tat peptide," *Biomaterials* **31**(4), 769–778 (2010).
8. K. Ino, M. Okochi, and H. Honda, "Application of magnetic force-based cell patterning for controlling cell–cell interactions in angiogenesis," *Biotechnol. Bioeng.* **102**(3), 882–890 (2009).
9. J. Yan, M. C. Estévez, J. E. Smith, K. Wang, X. He, L. Wang, and W. Tan, "Dye-doped nanoparticles for bioanalysis," *Nanotoday* **2**(3), 44–50 (2009).
10. J. H. Chang, K. H. Kang, J. Choi, and Y. K. Jeong, "High efficiency protein separation with organosilane assembled silica coated magnetic nanoparticles," *Superlattices Microstruct.* **44**(4-5), 442–448 (2008).
11. S. Ben-David Makhluf, R. Abu-Mukh, S. Rubinstein, H. Breitbart, and A. Gedanken, "Modified PVA–Fe_3O_4 nanoparticles as protein carriers into sperm cells," *Small* **4**(9), 1453–1458 (2008).
12. M. Higuchi, K. Ushiba, and M. Kawaguchi, "Structural control of peptide-coated gold nanoparticle assemblies by the conformational transition of surface peptides," *J. Colloid Interface Sci.* **308**(2), 356–363 (2007).
13. I. E. Sendroiu and R. M. Corn, "Nanoparticle diffraction gratings for DNA detection on photopatterned glass substrates," *BioInterphases* **3**(3), FD23–FD29 (2008).
14. R. Fernandez-Montesinos, P. M. Castillo, R. Klippstein, E. Gonzalez-Rey, J. A. Mejias, A. P. Zaderenko, and D. Pozo, "Chemical synthesis and characterization of silver-protected vasoactive intestinal peptide nanoparticles," *Nanomedicine* **4**(8), 919–930 (2009).
15. V. S. Y. Lin, K. Motesharei, K.-P. S. Dancil, M. J. Sailor, and M. R. Ghadiri, "A porous silicon-based optical interferometric biosensor," *Science* **278**, 840–843 (1997).
16. J. Rosenholm, C. Sahlgren, and M. Lindén, "Cancer-cell targeting and cell-specific delivery by mesoporous silica nanoparticles," *J. Mater. Chem.* **20**, 2707–2713 (2010).
17. G. Palestino, V. Agarwal, R. Aulombard, E. Pérez, and S. Gergely, "Biosensing and protein fluorescence enhancement by functionalized porous silicon devices," *Langmuir* **24**(23), 13765–13771 (2008).
18. L. Koker and K. W. Kolasinski, "Photoelectrochemical etching of Si and porous Si in aqueous HF," *Phys. Chem. Chem. Phys.* **2**, 277–281 (2000).
19. F. Michelotti, B. Sciacca, L. Dominici, M. Quaglio, E. Descovi, F. Giorgis, and F. Geobaldo, "Fast optical vapour sensing by Bloch surface waves on porous silicon membranes," *Phys. Chem. Chem. Phys.* **2**, 502–506 (2010).
20. D. Gallach, G. Recio Sánchez, A. Muñoz Noval, M. Manso Silván, G. Ceccone, R. J. Martín Palma, V. Torres Costa, and J. M. Martínez Duart, "Functionality of porous silicon particles: surface modification for biomedical applications," *Mater. Sci. Eng., B* **169**(1-3), 123–127 (2010).
21. C. Lee, H. Kim, C. Hong, M. Kim, S. S. Hong, D. H. Lee, and W. I. Lee, "Porous silicon as an agent for cancer thermotherapy based on near-infrared light irradiation," *J. Mater. Chem.* **18**, 4790–4795 (2008).
22. K. Rumpf, P. Granitzer, P. Pölt, S. Šimić, M. Hofmayer, and H. Krenn, "A ferromagnetic (porous silicon/metal)-nanocomposite with an additional paramagnetic behavior," *Physica E (Amsterdam)* **40**(7), 2517–2520 (2008).
23. K. Fukami, Y. Tanaka, M. L. Chourou, T. Sakka, and Y. H. Ogata, "Filling of mesoporous silicon with copper by electrodeposition from an aqueous solution," *Electrochim. Acta* **54**(8), 2197–2202 (2009).
24. L. Cheng, E. Anglin, F. Cunin, D. Kim, M. J. Sailor, I. Falkenstein, A. Tammewar, and W. R. Freeman, "Intravitreal properties of porous silicon photonic crystals: a potential self-reporting intraocular drug-delivery vehicle," *Br. J. Ophthalmol.* **92**(5), 705–711 (2008).
25. S. P. Low, N. H. Voelcker, L. T. Canham, and K. A. Williams, "The biocompatibility of porous silicon in tissues of the eye," *Biomaterials* **30**(15), 2873–2880 (2009).
26. H. Y. Lee, N. H. Lim, J. A. Seo, S. H. Yuk, B. K. Kwak, G. Khang, H. B. Lee, and S. H. Cho, "Preparation and magnetic resonance imaging effect of polyvinylpyrrolidone-coated iron oxide nanoparticles," *J. Biomed. Mater. Res., Part B: Appl. Biomater.* **79B**(1), 142–150 (2006).
27. A. Ciszewski, S. Posluszny, G. Milczarek, and M. Baraniak, "Effects of saccharin and quaternary ammonium chlorides on the electrodeposition of nickel from a Watts-type electrolyte," *Surf. Coat. Technol.* **183**(2-3), 127–133 (2004).
28. R. Oriňáková, A. Turoňová, D. Kladeková, M. Gálová, and R. M. Smith, "Recent developments in the electrodeposition of nickel and some nickel-based alloys," *J. Appl. Electrochem.* **36**(9), 957–972 (2006).
29. D. P. Lennon, S. E. Haynesworth, S. P. Bruder, N. Jaiswal, and A. I. Caplan, "Human and animal mesenchymal progenitor cells from bone marrow: identification of serum for optimal selection and proliferation," *In Vitro Cell. Dev. Biol.: Anim.* **32**(10), 602–611 (1996).
30. M. Manso, S. Ogueta, J. Pérez-Rigueiro, J. P. García, and J. M. Martínez-Duart, "Testing biomaterials by the in-situ evaluation of cell response," *Biomol. Eng.* **19**(2-6), 239–242 (2002).
31. R. J. Martín-Palma, L. Pascual, P. Herrero, and J. M. Martínez-Duart, "Direct determination of grain sizes, lattice parameters, and mismatch of porous silicon," *Appl. Phys. Lett.* **81**(1), 25–27 (2002).

32. Y.-M. Kwon, Z. Xia, S. Glyn-Jones, D. Beard, H. S. Gill, and D. W. Murray, "Dose-dependent cytotoxicity of clinically relevant cobalt nanoparticles and ions on macrophages *in vitro*," *Biomed. Mater.* **4**, 5002 (2009).
33. A. G. Roca, M. P. Morales, K. O'Grady, and C. J. Serna, "Structural and magnetic properties of uniform magnetite nanoparticles prepared by high temperature decomposition of organic precursors," *Nanotechnology* **17**(11), 2783–2788 (2006).
34. N. Deo, M. F. Bain, J. H. Montgomery, and H. S. Gamble, "Study of magnetic properties of thin cobalt films deposited by chemical vapour deposition," *J. Mater. Sci.: Mater. Electron.* **16**(7), 387–392 (2005).
35. H. Luo, D. Wang, J. He, and Y. Lu, "Magnetic Cobalt Nanowire Thin Films," *J. Phys. Chem. B* **109**(5), 1919–1922 (2005).
36. Y. Cedeño-Mattei and O. Perales-Perez, "Synthesis of high-coercivity cobalt ferrite nanocrystals," *Microelectron. J.* **40**(4-5), 673–676 (2009).
37. B. Feng, R. Y. Hong, L. S. Wang, L. Guo, H. Z. Li, J. Ding, Y. Zheng, and D. G. Wei, "Synthesis of Fe_3O_4/APTES/PEG diacid functionalized magnetic nanoparticles for MR imaging," *Colloids Surf., A* **328**(1-3), 52–59 (2008).
38. Z. Ma, Y. Guan, and H. Liu, "Superparamagnetic silica nanoparticles with immobilized metal affinity ligands for protein adsorption," *J. Magn. Magn. Mater*. **301**(2), 469–477 (2006).
39. H. Tamura, M. Rückschloss, T. Wirschem, and S Vepimageek, "On the possible origin of the photoluminescence from oxidized nanocrystalline silicon," *Thin Solid Films* **255**(1-2), 92–95 (1995).
40. Y. Kanemitsu, H. Uto, Y. Masumoto, T. Matsumoto, T. Futagi, T. Matsumoto, and H. Mimura, "Microstructure and optical properties of free-standing porous silicon films: size dependence of absorption spectra in Si nanometer-sized crystallites," *Phys. Rev. B* **48**(4), 2827–2830 (1993).
41. M. T. Kelly and A. B. Bocarsly, "Mechanisms of photoluminescent quenching of oxidized porous silicon applications to chemical sensing," *Coord. Chem. Rev.* **171**(1), 251–259 (1998).